

No-Touch Radiofrequency Ablation: A Comparison of Switching Bipolar and Switching Monopolar Ablation in *Ex Vivo* Bovine Liver

Won Chang, MD¹, Jeong Min Lee, MD^{1, 2}, Sang Min Lee, MD¹, Joon Koo Han, MD^{1, 2}

¹Department of Radiology, Seoul National University Hospital, Seoul 03080, Korea; ²Institute of Radiation Medicine, Seoul National University College of Medicine, Seoul 03080, Korea

Objective: To evaluate the feasibility, efficiency, and safety of no-touch switching bipolar (SB) and switching monopolar (SM) radiofrequency ablation (RFA) using *ex vivo* bovine livers.

Materials and Methods: A pork loin cube was inserted as a tumor mimicker in the bovine liver block; RFA was performed using the no-touch technique in the SM (group A1; 10 minutes, n = 10, group A2; 15 minutes, n = 10) and SB (group B; 10 minutes, n = 10) modes. The groups were compared based on the creation of confluent necrosis with sufficient safety margins, the dimensions, and distance between the electrode and ablation zone margin (DEM). To evaluate safety, small bowel loops were placed above the liver surface and 30 additional ablations were performed in the same groups.

Results: Confluent necroses with sufficient safety margins were created in all specimens. SM RFA created significantly larger volumes of ablation compared to SB RFA (all $p < 0.001$). The DEM of group B was significantly lower than those of groups A1 and A2 (all $p < 0.001$). Although thermal injury to the small bowel was noted in 90%, 100%, and 30% of the cases in groups A1, A2, and B, respectively, full depth injury was noted only in 60% of group A2 cases.

Conclusion: The no-touch RFA technique is feasible in both the SB and SM modes; however, SB RFA appears to be more advantageous compared to SM RFA in the creation of an ablation zone while avoiding the unnecessary creation of an adjacent parenchymal ablation zone or adjacent small bowel injuries.

Keywords: Minimally invasive; Bovine; Preclinical; Radiofrequency ablation; No-touch technique; Hepatocellular carcinoma

INTRODUCTION

Radiofrequency ablation (RFA) is the most widely used percutaneous thermal ablation technique for treating

Received August 20, 2016; accepted after revision October 12, 2016.

This study was partly supported by research fund from the STARmed Co. (No. 06-2016-0590).

Corresponding author: Jeong Min Lee, MD, Department of Radiology, Seoul National University Hospital, 101 Daehak-ro, Jongno-gu, Seoul 03080, Korea.

• Tel: (822) 2072-2584 • Fax: (822) 743-6385

• E-mail: leejm@radcom.snu.ac.kr

This is an Open Access article distributed under the terms of the Creative Commons Attribution Non-Commercial License (<http://creativecommons.org/licenses/by-nc/4.0>) which permits unrestricted non-commercial use, distribution, and reproduction in any medium, provided the original work is properly cited.

primary and metastatic hepatic tumors; it is widely accepted as a potential curative treatment option for early stage hepatocellular carcinoma (HCC) in nonsurgical candidates (1-4). However, RFA has a higher local tumor progression rate compared to surgery (5, 6). Typically, RFA is executed by deploying a monopolar multi-tined or internally cooled electrode into the tumor under the guidance of imaging modalities such as ultrasonography or computed tomography. With the existing single monopolar electrodes, the generation of a sufficient ablation volume including the tumor and a sufficient peritumoral margin (> 5 mm) is not always possible, and requires multiple overlapping ablations (7). To ensure larger or more uniform ablation zones, substantial efforts have been made for improving ablation systems, such as the development of the switching monopolar (SM) or multipolar approach; the modulation of

tissue characteristics including tissue perfusion, thermal, or electrical conductivity; and the combination of RFA with other therapies such as arterial embolization or liposomal doxorubicin (7-13). However, they inevitably increased complexity, complications, and potential toxicity of any compound regimen, and therefore, limitations in clinical efficacy persist (7). Furthermore, with multiple overlapping ablations, tumor seeding along the puncture route, particularly for tumors located on the liver surface, is another concern of the conventional RFA, although this risk can be lowered by tract ablation (14-18).

Recently, a few studies (19-22) demonstrated that multipolar RFA with multiple electrodes could be used for "no-touch" techniques and achieved promising results of high technical success rate, local tumor progression-free survival rate, and no tract seeding episodes in patients with HCCs. Because no-touch RFA is performed by inserting multiple electrodes outside tumors, thus avoiding a direct puncture to the tumors, the risk of tract seeding must be extremely low. However, to create complete necrosis of the target tumor between the electrodes, the mean ablation time was kept relatively long (18.5–27.2 minutes) and a large amount of radiofrequency (RF) energy had to be delivered, which resulted in a large ablation zone outside of the target tumor (19-22). In fact, theoretically, the deposition of a high density current into the target tissue including the tumor would be more easily achievable in the bipolar mode than in the monopolar mode having a centrifugal current flow from the electrode, which might reduce the ablation of the tissue positioned lateral to the electrodes (7). Although multipolar or switching bipolar (SB) RFA has been used for achieving no-touch ablation efficiency (23-25), no study has compared the monopolar and bipolar modes for the no-touch technique to date.

Therefore, we attempted to evaluate the *ex vivo* feasibility, efficiency, and safety of the no-touch technique in SB and SM modes using a separable clustered multiple electrode and a prototype RFA system that allows the automatic switching of RF energy delivery among the electrodes in either the bipolar or monopolar modes based on impedance spikes.

MATERIALS AND METHODS

The RFA System

To perform bipolar RFA, we developed a prototype of the multichannel RF system that allowed the automatic

switching of RF energy delivery among the three electrodes depending on impedance changes in both the monopolar and bipolar modes. In the monopolar mode, the switching between multiple electrodes occurred depending on impedance changes to use the inherent off time of the power pulsing algorithm to deliver energy through another electrically independent electrode, and similarly, the bipolar mode switching between one of the electrode pairs occurred depending on the impedance spikes (7, 10, 26). In both the SM and SB modes, if the impedance of one of the electrodes or one of the electrode pairs increased to 50 Ohm above the baseline impedance, the energy delivery switched automatically to the other electrode or other electrode pair (27). We used a separable clustered electrode (Octopus® electrode; STARmed, Goyang, Korea) with three internally cooled electrodes, each with a 2.5-cm long active tip for the no-touch technique (27).

We maintained each tip temperature below 25°C by infusing the normal saline solution at 0°C into the lumen of each electrode using a peristaltic pump (VIVA Pump; STARmed). We continuously monitored the technical parameters, such as power output, impedance, applied currents, and total delivered energy, and recorded them using VIVA Monitor Software V 1.0 (STARmed).

The *Ex Vivo* Experimental Setting

We separately performed two-phase experimental studies to evaluate the efficacy and safety of the SM and SB modes of the no-touch RFA technique.

In the first experiment, to compare the efficacies of the SM- and SB-RFA techniques, we prepared 30 bovine liver blocks, slicing each explanted bovine liver into 12 x 12 x 7-cm³ liver blocks. After we made a small incision at the center of each liver block, we inserted a 1.2 x 1.2 x 1.2-cm³ pork loin cube with an approximate diagonal line length of 2 ($1.2 \times \sqrt{3} \approx 2.0$) cm as a tumor mimicker while maintaining its diagonal line as parallel to the liver surface as possible. Subsequently, we placed each of the Octopus electrodes meticulously using the no-touch technique in a triangular array with a 2.5-cm inter-electrode distance through an acrylic plate that contained multiple holes at 5-mm intervals (27). Three electrodes were inserted at the same depth (4–5 cm) in the liver. We inserted a thermometer at the center of the ablation zone to monitor the tissue temperature in real time. Subsequently, we performed the RFA after immersing a liver block in a 50 x 20 x 25-cm³ saline-filled bath at room temperature. We then

No-Touch Radiofrequency Ablation Using Multiple Electrodes

recorded the elapsed times to reach 50, 60, 70, 80, and 90°C of tissue temperature.

In the second experiment, to evaluate the safety of SM- and SB-RFA, we checked the presence of organ injury as a safety parameter. Specifically, we prepared 30 additional 10 x 8 x 7.5-cm³ bovine liver blocks and immersed them in a 30 x 20 x 20-cm³ saline-filled bath. We inserted electrodes in a triangular array using the same acrylic plate with a 2.5-cm inter-electrode distance and placed one of the electrodes 14 mm below the upper surface of the liver; subsequently, we placed bovine small bowel loops just above the liver block (Fig. 1). We then placed a thermometer between the liver and small bowel loops and recorded the temperature; we also measured the surface temperature of the small bowel in contact with the liver surface using a thermal imaging camera (Fluke Ti90; Fluke Corp., Everett, WA, USA) at the end of each ablation.

Ablation Protocols

In each experiment, we performed 30 ablations. In the SM mode, RF energy (maximum 200 W) was delivered to one of the three electrodes and was automatically switched among the three electrodes depending on the elevation of the tissue impedance for 10 minutes (group A1, n = 10) or 15 minutes (group A2, n = 10). In the SB mode, the RF energy (maximum 100 W) was delivered to one of the electrode pairs and was switched in the same manner for 10 minutes (group B, n = 10) (Fig. 2). The 10-minute ablation time in the SB mode was based on previous studies that reported that bipolar RFA could be performed with relatively faster ablation and monopolar RFA (7, 23, 25). Therefore, we evaluated the ablative efficiency of the SM mode in two groups using the same as well as a longer duration than the SB mode in groups A1 and A2 (10 and 15 minutes, respectively) (23, 25).



Fig. 1. Ex vivo study to evaluate adjacent bowel injury during RFA. Photograph shows segment of small bowel wall neighboring upper surface of liver block that was dipped into 30 x 20 x 20-cm³ saline-filled acrylic bath at room temperature. Note that one of Octopus electrodes is inserted into bovine liver 14 mm below liver upper surface, and thermocouple is placed between small bowel wall and liver surface for real time temperature measurement.

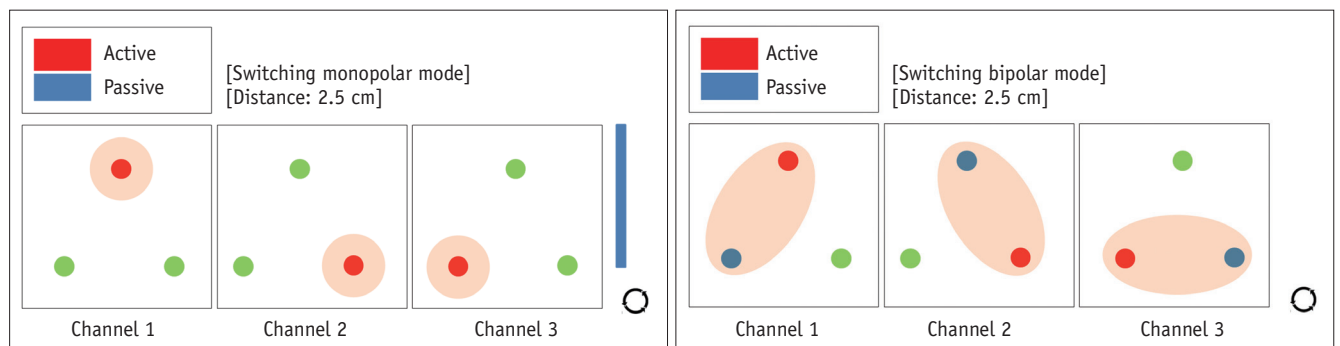


Fig. 2. Diagram showing typical patterns of switching monopolar and switching bipolar modes. In switching bipolar mode, pair of electrodes is activated.

Size Measurement and Shape Analysis of the Ablation Zones

We cut the ablated bovine liver blocks along the electrode tract and sliced in the transverse plane perpendicular to the axis of the electrode tracks. We considered the ablation technically successful when the RF-induced ablation zone showed > 5-mm peritumoral ablation margins outside the tumor mimicker in all dimensions of the slices (28-30). To prevent any bias in the ablation size measurements, we photographed the slices alongside a ruler on a copy stand using a digital camera (Nikon Coolpix S6900; Nikon Inc., Tokyo, Japan). Two observers (blinded, with 5 years of experience in the RFA procedure and experiments, and a technician with 10 years of experience in RFA experiments) measured the vertical diameter (Dv) at the vertical plane as well as the long-axis diameter (Dmx) and the short-axis diameter (Dmi) of the RF-induced ablation zones at the transverse plane with the maximum area on consensus (31). Furthermore, we measured the distances between the electrode and the outer margin of the ablation zone (DEM) on the same plane and calculated the mean value of the three DEMs (Fig. 3). We also measured all diameters and distances of the ablation zone including the central white and peripheral red zones. We performed all measurements on image files of the slices using Image J software (<https://imagej.nih.gov>) and calculated the volume of the ablation zone using the following formula by approximating the shape of the lesion to an ellipsoid: $\pi (Dv \times Dmx \times Dmi) / 6$. In case the ablation zone was non-confluent, we drew an ellipse intersected by the tangent points of the coagulation zone; we also measured the maximum (Dmx-eff) and minimum (Dmi-eff) diameters of the ellipse. We evaluated

the volumes of the ablation zones using the following formula according to the same approximation of the shape to an ellipsoid: $\text{Volume} = \pi / 6 \times Dmx\text{-eff} \times Dmi\text{-eff} \times Dv$, and we calculated the effective ablation volumes (Volume-eff) using the formula: $\text{Volume-eff} = \pi / 6 \times Dmi^3$, where Dmi was the shortest diameter among all the measured ones.

We quantitatively evaluated the shape of the RF-induced ablation zone using the ratio between the Dmi and Dmx and the circularity defined by the following formula: $\text{Circularity} = 4\pi A / P^2$, where A was the area of the measured zone and P was the perimeter of the area (25); we obtained this value by drawing the region of interest along the ablation margin on a transverse plane using the Image J software.

Assessing Thermal Injury to the Small Bowel

In the second experiment, we immediately checked the presence of small bowel injury after the ablation procedure to evaluate adjacent organ injury; we fixed injured bowel segments or bowel segments that most closely neighbored the ablation zone in 40 g/L formaldehyde solution, cut them into 3-mm thick slices, embedded them in paraffin, and stained them with hematoxylin and eosin for light microscopy. We graded the presence and depth of thermal injury to the small bowel as follows: 0, no injury; 1, partial thickness injury of the muscular layer; and 2, full thickness injury of the small bowel wall including mucosal injury (32, 33).

Statistical Analysis

For each *ex vivo* experiment, the results are presented as the mean \pm standard deviation (SD). We then compared

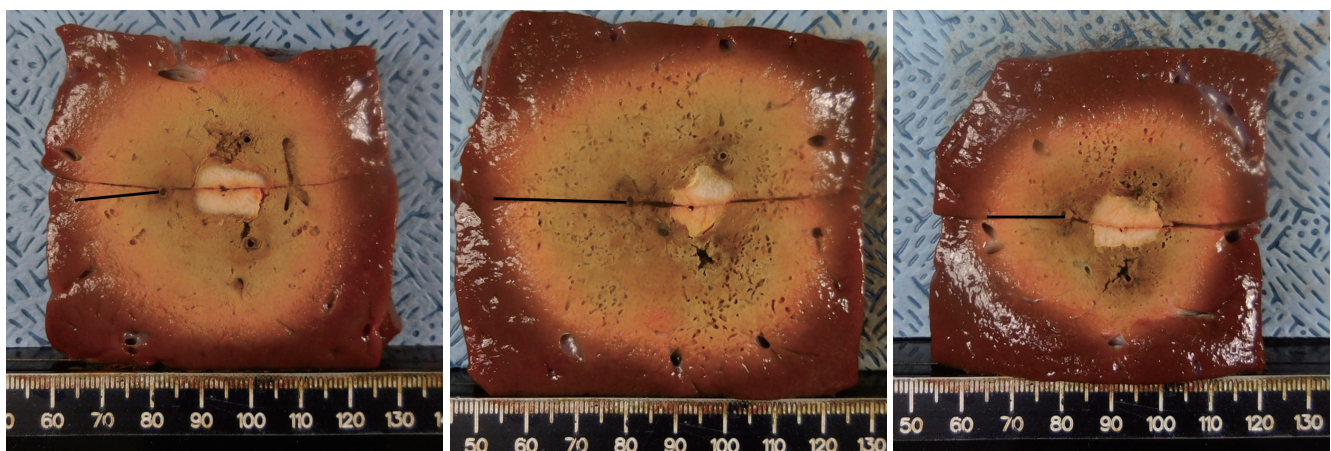


Fig. 3. Comparison of radio frequency ablation (RFA)-induced coagulation.

Transverse cut surfaces of ablated specimens in groups A1, A2, and B, respectively. Black bars indicate distance between outer margin of ablation zone and electrode.

the measured values and the technical parameters of the three groups (A1 vs. A2 vs. B) using analysis of variance (ANOVA), using Bonferroni correction for post hoc analysis. To compare the variability of the ablation volume among the three groups, we calculated the coefficient of variation of the ablation volume as the ratio of the SD to the mean volume of the ablation zone. Regarding the proportion of the organ injury, we used the chi-squared test. For the ANOVAs, we considered p values < 0.05 statistically significant, and for the multiple pairwise comparisons between two groups, we considered p values < 0.017 statistically significant by Bonferroni correction. We performed all statistical analyses using MedCalc statistical software, version 12.2.1 (MedCalc Software, Mariakerke, Belgium).

RESULTS

Technical Parameters

The mean impedance of the SB mode was significantly

higher than that of the SM mode (all $p < 0.001$) (Table 1), and the mean delivered RF power and total amounts of delivered energy were also significantly lower in the SB mode than in the SM mode (all $p < 0.001$).

Technical Success, Ablation Size Measurement, and Shape Analysis

None of the specimens showed technical failure or partial confluent or separated ablation (Table 2, Fig. 3).

Ablation Size Measurements

The mean Dmi of the ablation areas in groups A1, A2, and B were 4.98 ± 0.23 , 5.24 ± 0.26 , and 4.49 ± 0.13 cm, respectively ($p < 0.001$) (Table 3). The SM-RFA (groups A1 and A2) generated significantly larger gross ablation volumes than SB-RFA (group B): group A1: 65.9 ± 8.6 cm³; group A2: 73.6 ± 10.0 cm³; and group B: 52.1 ± 5.0 cm³ ($p < 0.001$). The effective ablation volumes were 57.7 ± 9.8 , 57.9 ± 7.3 , and 46.8 ± 3.1 cm³ in groups A1, A2, and B, respectively, and were significantly larger for SM-RFA than

Table 1. Measured Values of Technical Parameters According to Power Application Modes

Parameters	Group A1 (n = 10)	Group A2 (n = 10)	Group B (n = 10)	P	A1 vs. A2	A1 vs. B	A2 vs. B
Total delivered energy (Kcal)	12.0 ± 0.8	14.6 ± 1.3	9.0 ± 0.9	< 0.001	< 0.001	< 0.001	< 0.001
Average watt (W)	110.8 ± 6.1	95.5 ± 6.4	77.6 ± 5.2	< 0.001	< 0.001	< 0.001	< 0.001
Impedance (Ohm)	58.8 ± 1.4	61.5 ± 1.6	93.6 ± 12.4	< 0.001	0.001	< 0.001	< 0.001

Table 2. Results of Technical Success Rate, and Shape Analysis of RF-Induced Ablation Zones in Each Group

Parameters	Group A1 (n = 10)	Group A2 (n = 10)	Group B (n = 10)	P
Qualitative analysis of ablation, %				
Technical success	100 (10/10)	100 (10/10)	100 (10/10)	1
Confluent ablation	100 (10/10)	100 (10/10)	100 (10/10)	1
Partial confluent ablation	0 (0/10)	0 (0/10)	0 (0/10)	1
Separated ablation	0 (0/10)	0 (0/10)	0 (0/10)	1
Quantitative analysis of coagulation necrosis				
Circularity	0.95 ± 0.05	0.97 ± 0.01	0.94 ± 0.06	0.334
Dmi/Dmx ratio	0.95 ± 0.04	0.94 ± 0.04	0.94 ± 0.04	0.795

Dmi = minimum diameter of the ablative zone, Dmx = maximum diameter of the ablative zone

Table 3. Results of Ablation Size Measurement in Each Group

Parameters	Group A1 (n = 10)	Group A2 (n = 10)	Group B (n = 10)	P	A1 vs. A2	A1 vs. B	A2 vs. B
Dmx (cm)	5.24 ± 0.23	5.58 ± 0.29	4.78 ± 0.20	< 0.001	0.01	< 0.001	< 0.001
Dmi (cm)	4.98 ± 0.23	5.24 ± 0.26	4.49 ± 0.13	< 0.001	0.03	< 0.001	< 0.001
Dv (cm)	4.81 ± 0.29	4.79 ± 0.20	4.63 ± 0.24	0.384			
Gross ablation volume (cm ³)	65.9 ± 8.6	73.6 ± 10.0	52.1 ± 5.0	< 0.001	0.083	0.001	< 0.001
Effective ablation volume (cm ³)	57.7 ± 9.8	57.9 ± 7.3	46.8 ± 3.1	< 0.001	0.963	0.006	< 0.001
DEM (cm)	1.67 ± 0.10	1.86 ± 0.18	1.39 ± 0.08	< 0.001	0.013	< 0.001	< 0.001
CV of volume (%)	13	13.6	9.6				

CV = coefficient of variation, DEM = distance between electrode and ablation zone margin, Dmi = minimum diameter of the ablative zone, Dmx = maximum diameter of the ablative zone, Dv = vertical diameter of the ablative zone

for SB-RFA (A1 vs. B, $p = 0.006$; A2 vs. B, $p < 0.001$).

Ablation Shape Analysis

The circularities of the ablative zones were 0.95 ± 0.05 in group A1, 0.97 ± 0.01 in group A2, and 0.94 ± 0.06 in group B ($p = 0.334$), suggesting that there were no significant differences in the quantitative values of the shape analysis among the three groups; however, DEM was significantly lower in group B (1.39 ± 0.08 cm) than in groups A1 (1.67 ± 0.10 cm) and A2 (1.86 ± 0.18 cm) ($p < 0.001$).

Elapsed Time

He elapsed times to reach 60, 70, 80, and 90°C were significantly faster in the SB-RFA group than in the SM-RFA group (groups A1 and A2: $p = 0.002$ for 60°C; $p < 0.001$ for 70, 80, and 90°C; $p = 0.681$ for 50°C) (Table 4).

The Second Experiments

We noted thermal injury to the small bowel in 90% (9/10), 100% (10/10), and 30% (3/10) of the cases in groups A1, A2, and B, respectively (A1 vs. B, $p = 0.008$; A2 vs. B, $p = 0.001$; A1 vs. A2, $p = 0.317$) (Fig. 4). We observed six cases of grade 2 small bowel injury only in group A2 (6/10), and all thermal injuries of the small bowel noted in group A1 and B were grade 1 (A2 vs. A1 and B for grade 2 injury, $p = 0.004$). The mean final temperatures measured by a thermocouple placed between the liver surface and the small bowel after the completion of ablation were 59.1 ± 7.4 , 65.1 ± 8.6 , and 49.4 ± 6.7 °C in groups A1, A2, and B, respectively. The surface temperatures of the small bowel neighboring the ablation zone measured by a thermal imaging camera were also significantly lower in the SB group than in the SM groups and significantly lower in group A1 than in group A2 (all $p < 0.001$): 48.4 ± 3.1 , 56.7 ± 3.5 , and 40.5 ± 2.3 °C in groups A1, A2, and B, respectively.

DISCUSSION

The present *ex vivo* study demonstrated that no-touch RFA using an Octopus electrode in both the SM and SB modes was feasible for treating 2 cm tumors. Furthermore, the ablation volume of SM-RFA was significantly larger than that of SB-RFA with similar circularity; however, SM mode also showed greater ablation of the liver tissue outside of the electrode (greater DEM). On the contrary, the temperature at the center of the ablation zone rose more quickly in the SB mode than in the SM mode. The results of the present study could be attributed to the basic difference between the SM and SB modes in terms of electrical current flow; in monopolar RFA, the current spreads from each electrode centrifugally to the periphery, whereas during bipolar RFA, the electric current flows between a pair of electrodes and prevents the ablation zone from perfusion-mediated cooling, resulting in faster and more focal heating between the electrodes (7, 25). Although there was no technical failure and no non-confluent coagulation in either the SM or SB modes, bipolar RFA was less affected by the heat sink phenomenon than was monopolar RFA in the perfused *ex vivo* bovine liver model (34). However, irrespective of the multiple advantages conferred by the SB mode for no-touch RFA, there might be some potential disadvantages, including the requirement for more precise placement of the electrodes to produce a confluent zone of necrosis and greater difficulty controlling impedance than the SM mode by local conductivity changes that result from the ablation (7). Therefore, regarding the feasibility of the percutaneous no-touch RFA technique, the use of SB-RFA should be validated in *in vivo* studies.

The SB mode showed significantly smaller DEM than did the SM mode, which might indicate less injury to the adjacent liver parenchyma using no-touch RFA. Furthermore, the present study also demonstrated that no-touch RFA in the SB mode generated small bowel injury less frequently than in the SM mode and caused less tissue temperature elevation from the adjacent small bowel wall.

Table 4. Elapsed Times to Reach Specific Temperatures in Each Group

Temperature	SM-RFA (Seconds)	SB-RFA (Seconds)	P
50°C	83.1 ± 22.8	80.8 ± 5.6	0.681
60°C	109.1 ± 14.5	96.2 ± 6.0	0.002
70°C	130.1 ± 15.2	108.6 ± 7.8	< 0.001
80°C	154.0 ± 18.5	121.6 ± 9.6	< 0.001
90°C	185.6 ± 26.0	137.9 ± 11.8	< 0.001

RFA = radiofrequency ablation, SB = switching bipolar, SM = switching monopolar

No-Touch Radiofrequency Ablation Using Multiple Electrodes

As a secondary safety parameter, we evaluated DEM in the ablation zones and measured tissue temperature from the area between the bowel and the liver capsule above the ablation zone. Therefore, based on our study results, we believe that the SB mode might exhibit a better safety profile than the SM mode during no-touch RFA.

Conventional monopolar technique requires precise placement of the electrode within the target tumor, ideally along the its central axis because it creates an ablation zone from the center of the tumor to the periphery owing to the condensed deposition of electrical current in the tissue surrounding the electrode. Therefore, there might be some risk of track seeding or peritoneal seeding after RFA

and a relatively higher risk of local recurrence related to the failure to generate a sufficient safety margin around the tumor (16). Indeed, there is a trade-off between generating a sufficient peritumoral margin to lower recurrence after RFA and preventing unintended adjacent thermal injury. Moreover, after Llovet et al. (35) reported a high rate (12.5%) of tumor tract seeding in 32 patients with HCC who had been treated with RFA; with increased use, tumor tract seeding after percutaneous RFA was found to be a major issue, particularly in patients with a curative chance (36). However, according to a recent systematic review of tumor seeding after percutaneous diagnostic and therapeutic approaches for HCC (15), the mean risk for seeding after

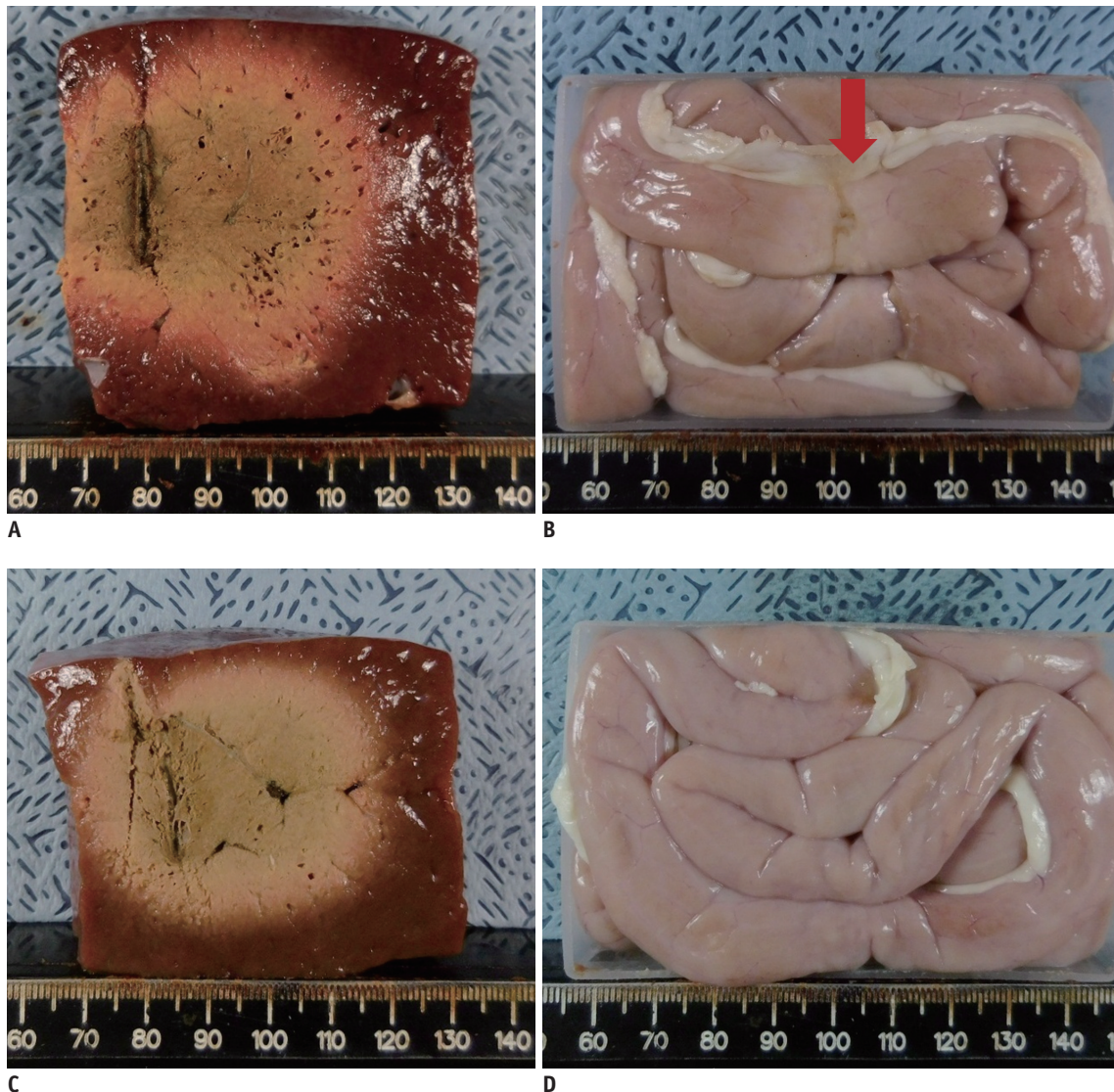


Fig. 4. Comparison of adjacent small bowel thermal injury during RFA in groups A2 and B.
A, B. Vertical cut surface of ablated specimens and adjacent small bowel in group A2. Note that ablated area extended to liver surface and there is color change of small bowel wall by thermal injury (arrow). **C, D.** Vertical cut surfaces of ablated specimens and adjacent small bowel in group B. Note that liver surface was not ablated and adjacent small bowel showed no thermal injury.

RFA alone was 1.73% (range, 0–5.56%), and after RFA with biopsy, the mean risk for seeding was 2.5%. Nonetheless, considering that immune suppression is essentially used for liver transplantation and waiting time for liver transplantation is quite long (usually longer than 1 year), when RFA is used to manage patients with liver cirrhosis and small HCCs, it would be ideal to avoid unnecessary liver parenchymal damage in the area surrounding the target tumor and also to avoid any risk of tumor seeding. In fact, the no-touch technique could be quite valuable for preventing track seeding after RFA, which is very important in patients who are on the waiting list for liver transplantation or patients with tumors located on the liver surface (36, 37). However, for no-touch RFA with multiple electrodes placed outside the tumor, the peritumoral ablation size could be larger than that for conventional RFA methods with tumor puncture. In the present study results, the SB mode showed less DEM than the SM mode. Therefore, we believe that the SB mode can be more optimal for no-touch RFA than the SM mode. Assuming that the ablation zone of each electrode in the SM-RFA is circular in the transverse plane, the diameter of ablation zone should be larger than interelectrode distance / $\sqrt{3}$ to induce non-separated coagulation. This indicates that the minimal DEM in the SM mode should be interelectrode distance / $\sqrt{3}$, and with a 2.5-cm interelectrode distance, the minimal DEM was approximately 1.4 cm. In the present study, the mean DEM values were larger than 1.4 cm in the SM mode (groups A1 and A2) and smaller than 1.4 cm in the SB mode (group B). Additionally, in the second experiment, to show the adjacent organ injury, we placed the electrode 1.4 cm below the liver surface considering the calculated minimal DEM.

The present study has a number of limitations. First, we established the initial feasibility and safety of *ex vivo* no-touch RFA using a newly developed RF generator with SB and SM modes was established, but, as previously mentioned, we might not have been able to properly assess various effects including the heat sink phenomenon and physical thermal insulation barriers such as the liver capsule. Second, we did not compare our SB-RFA system with the previously reported multipolar RFA systems that showed promising outcomes for no-touch ablation (22). Third, we only tested no-touch linear electrode insertion for maximum intervals of 25 mm; considering that there were no technical failures in generating confluent ablation in the three groups, additional examinations at larger inter-electrode intervals > 25 mm could be valuable. However,

we believe that the no-touch technique could be ideally applicable to small tumors *in vivo* in the human liver, likely with maximum diameters of 2–2.5 cm. Finally, we performed the RF ablations using a tumor mimicker model from a pork loin cube; therefore, the thermal efficiency of the current RF system in the present study might not translate into real clinical practice owing to the different tissue textures of target tumors.

In conclusion, our results demonstrated that the no-touch technique is feasible using both the SB and SM modes; however, SB-RFA may exhibit a better safety profile, a smaller adjacent parenchymal ablation zone, and less frequent adjacent small bowel injuries than SM-RFA.

Acknowledgments

We thank Dong Un Kim, BA and Jung Hyuk Zu, BA for his contribution for technical assistance for radiofrequency ablation experiments.

REFERENCES

1. Bruix J, Sherman M; American Association for the Study of Liver Diseases. Management of hepatocellular carcinoma: an update. *Hepatology* 2011;53:1020-1022
2. European Association for the Study of the Liver; European Organisation for Research and Treatment of Cancer. EASL-EORTC clinical practice guidelines: management of hepatocellular carcinoma. *J Hepatol* 2012;56:908-943
3. Salhab M, Canelo R. An overview of evidence-based management of hepatocellular carcinoma: a meta-analysis. *J Cancer Res Ther* 2011;7:463-475
4. Wu YZ, Li B, Wang T, Wang SJ, Zhou YM. Radiofrequency ablation vs hepatic resection for solitary colorectal liver metastasis: a meta-analysis. *World J Gastroenterol* 2011;17:4143-4148
5. Chen MS, Li JQ, Zheng Y, Guo RP, Liang HH, Zhang YQ, et al. A prospective randomized trial comparing percutaneous local ablative therapy and partial hepatectomy for small hepatocellular carcinoma. *Ann Surg* 2006;243:321-328
6. Wang JH, Wang CC, Hung CH, Chen CL, Lu SN. Survival comparison between surgical resection and radiofrequency ablation for patients in BCLC very early/early stage hepatocellular carcinoma. *J Hepatol* 2012;56:412-418
7. Ahmed M, Brace CL, Lee FT Jr, Goldberg SN. Principles of and advances in percutaneous ablation. *Radiology* 2011;258:351-369
8. Goldberg SN. Science to practice: which approaches to combination interventional oncologic therapy hold the greatest promise of obtaining maximal clinical benefit? *Radiology* 2011;261:667-669
9. Laeseke PF, Sampson LA, Haemmerich D, Brace CL, Fine JP, Frey TM, et al. Multiple-electrode radiofrequency ablation

- creates confluent areas of necrosis: in vivo porcine liver results. *Radiology* 2006;241:116-124
10. Lee JM, Han JK, Kim HC, Kim SH, Kim KW, Joo SM, et al. Multiple-electrode radiofrequency ablation of in vivo porcine liver: comparative studies of consecutive monopolar, switching monopolar versus multipolar modes. *Invest Radiol* 2007;42:676-683
 11. Lee ES, Lee JM, Kim KW, Lee IJ, Han JK, Choi BI. Evaluation of the in vivo efficiency and safety of hepatic radiofrequency ablation using a 15-G Octopus® in pig liver. *Korean J Radiol* 2013;14:194-201
 12. Wang X, Hu Y, Ren M, Lu X, Lu G, He S. Efficacy and safety of radiofrequency ablation combined with transcatheter arterial chemoembolization for hepatocellular carcinomas compared with radiofrequency ablation alone: a time-to-event meta-analysis. *Korean J Radiol* 2016;17:93-102
 13. Kim JW, Shin SS, Heo SH, Hong JH, Lim HS, Seon HJ, et al. Ultrasound-guided percutaneous radiofrequency ablation of liver tumors: how we do it safely and completely. *Korean J Radiol* 2015;16:1226-1239
 14. Hori T, Nagata K, Hasuike S, Onaga M, Motoda M, Moriuchi A, et al. Risk factors for the local recurrence of hepatocellular carcinoma after a single session of percutaneous radiofrequency ablation. *J Gastroenterol* 2003;38:977-981
 15. Stigliano R, Marelli L, Yu D, Davies N, Patch D, Burroughs AK. Seeding following percutaneous diagnostic and therapeutic approaches for hepatocellular carcinoma. What is the risk and the outcome? Seeding risk for percutaneous approach of HCC. *Cancer Treat Rev* 2007;33:437-447
 16. Imamura J, Tateishi R, Shiina S, Goto E, Sato T, Ohki T, et al. Neoplastic seeding after radiofrequency ablation for hepatocellular carcinoma. *Am J Gastroenterol* 2008;103:3057-3062
 17. Snoeren N, Jansen MC, Rijken AM, van Hillegersberg R, Slooter G, Klaase J, et al. Assessment of viable tumour tissue attached to needle applicators after local ablation of liver tumours. *Dig Surg* 2009;26:56-62
 18. Park SI, Kim IJ, Lee SJ, Shin MW, Shin WS, Chung YE, et al. Angled cool-tip electrode for radiofrequency ablation of small superficial subcapsular tumors in the liver: a feasibility study. *Korean J Radiol* 2016;17:742-749
 19. Seror O, N'Kontchou G, Van Nhieu JT, Rabahi Y, Nahon P, Laurent A, et al. Histopathologic comparison of monopolar versus no-touch multipolar radiofrequency ablation to treat hepatocellular carcinoma within Milan criteria. *J Vasc Interv Radiol* 2014;25:599-607
 20. Wu LW, Chen CY, Liu CJ, Chen MY, Liu PC, Liu PF, et al. Multipolar radiofrequency ablation with non-touch technique for hepatocellular carcinoma ≤ 3 cm: a preliminary report. *Adv Dig Med* 2014;1:80-85
 21. Hocquet A, Aubé C, Rode A, Cartier V, Sutter O, Manichon AF, et al. Comparison of no-touch multi-bipolar vs. monopolar radiofrequency ablation for small HCC. *J Hepatol* 2017;66:67-74
 22. Seror O, N'Kontchou G, Nault JC, Rabahi Y, Nahon P, Ganne-Carrié N, et al. Hepatocellular carcinoma within Milan criteria: no-touch multipolar radiofrequency ablation for treatment-long-term results. *Radiology* 2016;280:611-621
 23. Lee JM, Kim SH, Han JK, Sohn KL, Choi BI. Ex vivo experiment of saline-enhanced hepatic bipolar radiofrequency ablation with a perfused needle electrode: comparison with conventional monopolar and simultaneous monopolar modes. *Cardiovasc Intervent Radiol* 2005;28:338-345
 24. Osaki Y, Ikeda K, Izumi N, Yamashita S, Kumada H, Hatta S, et al. Clinical effectiveness of bipolar radiofrequency ablation for small liver cancers. *J Gastroenterol* 2013;48:874-883
 25. Yoon JH, Lee JM, Woo S, Hwang EJ, Hwang I, Choi W, et al. Switching bipolar hepatic radiofrequency ablation using internally cooled wet electrodes: comparison with consecutive monopolar and switching monopolar modes. *Br J Radiol* 2015;88:20140468
 26. Lee FT Jr, Haemmerich D, Wright AS, Mahvi DM, Sampson LA, Webster JG. Multiple probe radiofrequency ablation: pilot study in an animal model. *J Vasc Interv Radiol* 2003;14:1437-1442
 27. Yoon JH, Lee JM, Han JK, Choi BI. Dual switching monopolar radiofrequency ablation using a separable clustered electrode: comparison with consecutive and switching monopolar modes in ex vivo bovine livers. *Korean J Radiol* 2013;14:403-411
 28. Kim YS, Rhim H, Cho OK, Koh BH, Kim Y. Intrahepatic recurrence after percutaneous radiofrequency ablation of hepatocellular carcinoma: analysis of the pattern and risk factors. *Eur J Radiol* 2006;59:432-441
 29. Nakazawa T, Kokubu S, Shibuya A, Ono K, Watanabe M, Hidaka H, et al. Radiofrequency ablation of hepatocellular carcinoma: correlation between local tumor progression after ablation and ablative margin. *AJR Am J Roentgenol* 2007;188:480-488
 30. Kim YS, Lee WJ, Rhim H, Lim HK, Choi D, Lee JY. The minimal ablative margin of radiofrequency ablation of hepatocellular carcinoma (> 2 and < 5 cm) needed to prevent local tumor progression: 3D quantitative assessment using CT image fusion. *AJR Am J Roentgenol* 2010;195:758-765
 31. Ahmed M, Solbiati L, Brace CL, Breen DJ, Callstrom MR, Charboneau JW, et al. Image-guided tumor ablation: standardization of terminology and reporting criteria--a 10-year update. *Radiology* 2014;273:241-260
 32. Tulikangas PK, Smith T, Falcone T, Boparai N, Walters MD. Gross and histologic characteristics of laparoscopic injuries with four different energy sources. *Fertil Steril* 2001;75:806-810
 33. Martin KE, Moore CM, Tucker R, Fuchshuber P, Robinson T. Quantifying inadvertent thermal bowel injury from the monopolar instrument. *Surg Endosc* 2016;30:4776-4784
 34. Pillai K, Akhter J, Chua TC, Shehata M, Alzahrani N, Al-Alem I, et al. Heat sink effect on tumor ablation characteristics as observed in monopolar radiofrequency, bipolar radiofrequency, and microwave, using ex vivo calf liver

- model. *Medicine (Baltimore)* 2015;94:e580
35. Llovet JM, Vilana R, Brú C, Bianchi L, Salmeron JM, Boix L, et al. Increased risk of tumor seeding after percutaneous radiofrequency ablation for single hepatocellular carcinoma. *Hepatology* 2001;33:1124-1129
36. Cabibbo G, Craxi A. Needle track seeding following percutaneous procedures for hepatocellular carcinoma. *World J Hepatol* 2009;1:62-66
37. Kawamura Y, Ikeda K, Fukushima T, Hara T, Hosaka T, Kobayashi M, et al. Potential of a no-touch pincer ablation procedure for small hepatocellular carcinoma that uses a multipolar radiofrequency ablation system: an experimental animal study. *Hepatol Res* 2014;44:1234-1240